Melting modeling of mixed peridotitic and mafic lithologies at shallow depths of the continental metasomatized lithospheric mantle: Implementation for the Early Cretaceous volcanic rocks of Eastern Mongolia*

M. V. Kuznetsov[1], *V. M. Savatenkov*[1,2]

[1] Institute of Precambrian Geology and Geochronology
of the Russian Academy of Sciences,
2, nab. Makarova, St. Petersburg, 199034, Russian Federation
[2] St. Petersburg State University,
7–9, Universitetskaya nab., St. Petersburg, 199034, Russian Federation

For citation: Kuznetsov, M. V., Savatenkov, V. M. (2023). Melting modeling of mixed peridotitic and mafic lithologies at shallow depths of the continental metasomatized lithospheric mantle: Implementation for the Early Cretaceous volcanic rocks of Eastern Mongolia. *Vestnik of Saint Petersburg University. Earth Sciences*, 68 (3), 596–617. https://doi.org/10.21638/spbu07.2023.309

The Eastern Mongolia volcanic area formed in the Late Mesozoic — Early Cenozoic within Central Asian Orogenic Belt. The main volcanic events of the area occurred in the Early Cretaceous when alkaline basaltic lavas erupted and formed the so-called cover volcanic complex. Geochemical and isotope features of the cover volcanic complex allowed researchers to identify the following mantle rocks as their source: metasomatized peridotites, eclogites, and pyroxenites. Thermodynamic modeling in alphaMELTS program was performed to determine whether the simultaneous melting of these rocks with subsequent processes of crystallization differentiation could lead to the formation of the studied rocks. The modeling results show that the melting of the most enriched with incompatible trace elements peridotites, eclogites, and pyroxenites cannot produce the rocks of the cover volcanic complex. At the same time, the mixing of peridotite- and eclogite-derived melts corresponds most closely to the mechanism of rock formation. However, Ti, K, P, Rb, and Sr enrichment of the studied rocks also requires participation in magma generation processes of mantle metasomatic veins enriched with rutile, apatite, phlogopite, and amphibole.

Keywords: Eastern Mongolia, Early Cretaceous volcanism, thermodynamic modeling, eclogites, pyroxenites, mantle metasomatic veins.

1. Introduction

The Eastern Mongolia Volcanic Area (EMVA) is a part of a volcanic province formed during the Late Mesozoic — Early Cenozoic in the east of Asia within the Central Asian Orogenic Belt (CAOB). Despite its name, a small part of the area is located within Russia (Eastern Transbaikalia). The sources of the volcanic rock formation are still debatable. This is especially characteristic of the Early Cretaceous differentiated basaltic rocks ($SiO_2 \geq 47$ wt.%, $MgO \leq 4.5$ wt.%) of the area comprising the so-called cover volcanic

* This work was subsidized by the Russian Science Foundation (project no. 23-27-00165) and the State Assignments of Institute of Precambrian Geology and Geochronology of the Russian Academy of Sciences no. FMUW-2022-0005.

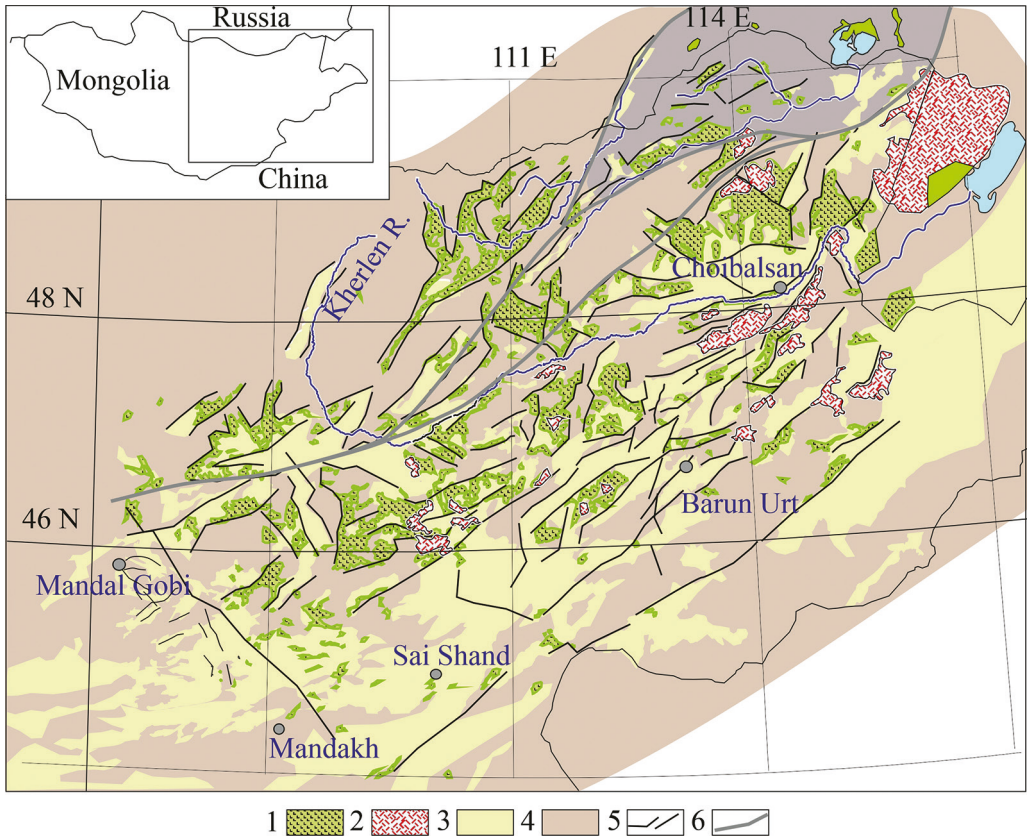

Fig. 1. Scheme of the Early Cretaceous volcanism (cover volcanic complex) within the Eastern Mongolia volcanic area. The upper inset shows the position of the area within Mongolia:

1 — predominantly basaltic lava, 2 — mainly trachyrhyodacite and trachyrhyolite lava, 3 — Cretaceous basins, 4 — pre-Cretaceous basement, 5 — faults, 6 — sutures of the Mongol — Okhotsk ocean

complex (Kuznetsov et al., 2022; Kuznetsov et al., 2023; Yarmolyuk et al., 2020) (Fig. 1). T. Sheldrick and the authors (Sheldrick et al., 2020a; Sheldrick et al., 2020b; Sheldrick et al., 2020c) identified eclogites, pyroxenites, and peridotites of the continental metasomatized lithospheric mantle (CMLM) as the sources of these rocks. Later (Kuznetsov et al., 2022) came to a similar conclusion using data on the rocks' Sr, Nd, and Pb isotope compositions.

Thus, previous studies suggest that the Early Cretaceous basalts of the EMVA were formed because of the simultaneous melting of the CMLM represented by peridotites, eclogites, and pyroxenites. However, these conclusions are based on comparing Mongolian volcanic rocks with well-studied most primitive rocks of other intraplate volcanic provinces. Such an approach has limitations because the variations in the chemical composition of volcanic rocks result at least from different degrees of melting and fractional crystallization. Not considering both factors can lead to incorrect estimates of the parental melts' compositions. Also, it is worth noting that only (Peretyazhko et al., 2018; Sheldrick et al., 2020a) tried to evaluate the role of melting and fractional crystallization using numerical modeling based on equations with fixed parameters (source mineralogy and

cumulate composition). However, these parameters change according to thermodynamic equilibrium conditions in the "restite — melt" or "cumulate — melt" systems in natural processes. Thus, a more rigorous approach is required to consider the magmatic system's thermodynamic features. Such an approach should use numerical thermodynamic modeling of phase equilibria in the magmatic system based on experimental data of the melting processes of different lithologies.

The numerical thermodynamic modeling was widely applied to the characterization of magmatic processes in recent decades through the use of alphaMELTS software package, which includes thermodynamic models of (Asimow and Ghiorso, 1998; Ghiorso et al., 2002; Ghiorso and Sack, 1995). It is an effective tool for a more realistic characterization of the influence of various processes (partial melting, fractional crystallization, assimilation, mixing, e. g.) on the evolution of the magmatic melts' composition.

Thus, the thermodynamic modeling approach (alphaMELTS) is used in this paper to determine whether the simultaneous melting of various CMLM lithologies produced parental magmas of the Early Cretaceous rocks of the EMVA.

2. Geological setting

The EMVA is similar in structure, development features, and composition of its magmatic products to other volcanic areas that occurred within the East Asia province (Fig. 1). The age of the volcanic fields of the EMVA spans from 140 to 48 Ma (Bars et al., 2018; Dash et al., 2015; Kuznetsov et al., 2022; Sheldrick et al., 2020a; Yarmolyuk et al., 2020), which corresponds to the Early Cretaceous — Early Cenozoic. However, this paper only considers the genesis of the Early Cretaceous volcanic rocks (140–100 Ma). Their structural features are discussed in detail in (Yarmolyuk et al., 2020; Kuznetsov et al., 2022). Further, we briefly summarize the main conclusions of these works.

The main structure-forming and volcanic events happened in the EMVA at the beginning of the Early Cretaceous. First, the structural framework of this area was formed, whose style is defined by a system of northeast-trending depressions and grabens. Second, mafic lavas formed a thick lava cover. This phase of volcanism (140–120 Ma) ended with felsic magmatism, which formed groups of large extrusions, small central volcanoes, and lava domes. In the second half of the Early Cretaceous (120–100 Ma), the lava piles of mafic rocks were formed only. Volcanic rocks are found in the area in various combinations, but the dominant rock associations are always basalt-trachybasalt-trachyandesite and rhyolite-trachyrhyolite. These rocks were produced during the main volcanic phase, encompassing most of the Early Cretaceous, and associated with active graben-forming processes. They dominate the area and make up its lava cover; hence (Kuznetsov et al., 2022; Yarmolyuk et al., 2020) refer to them as the cover volcanic complex (CVC).

The volcanic area was formed within a territory, including terranes of different origins and ages. However, most Early Cretaceous volcanic fields occurred within the Ereendavaa microcontinent. The rocks with high degrees of metamorphism, including granitic gneisses and migmatites (Badarch et al., 2002), previously justified the Paleoproterozoic age of the Ereendavaa. However, based on the dating of detrital zircons, L. Miao and autors (Miao et al., 2017) have suggested that the formation of the Ereendavaa occurred in the Paleozoic.

3. Methods

AlphaMELTS is a software package that allows modeling the phase (minerals and melts) relations in magmatic processes. It is based on an approach that assumes the minimization of the Gibbs energy in a system in thermodynamic equilibrium. AlphaMELTS can simulate partial melting, equilibrium crystallization, fractional crystallization, and assimilation using different thermodynamic algorithms. The task of alphaMELTS is to find a model where minerals and melts with specific chemical compositions coexist at minimum energy and given temperature (T) and pressure (P). The software package uses the thermodynamic data presented by (Berman, 1988).

We use the pMELTS algorithm of alphaMELTS in our calculations (Ghiorso et al., 2002). It is possible to calculate equilibrium phase relationships for magmatic systems in temperature range of 1000 to 2500 °C and pressure range of 10 to 30 kbar in pMELTS. This thermodynamic model was calibrated in the system SiO_2-TiO_2-Al_2O_3-Fe_2O_3-Cr_2O_3-FeO-MgO-CaO-Na_2O-K_2O-P_2O_5-H_2O. Therefore, using other oxides in modeling is unpredictable and not recommended.

It should be noted that the results of numerical calculations cannot strictly correspond to real natural processes. They are prognostic. In addition, pMELTS has significant limitations in the quantitative assessment of accessory phases (rutile, apatite, etc.), which are stable during the melting of mantle or crustal substrate and determine the behavior of trace elements in the resulting melts. Thus, modeling in pMELTS allows us to characterize the dominant trends in the chemical evolution composition of the formed melts, but these models do not describe magmatic processes accurately.

To determine the genesis of CVC rocks, pMELTS was used to simulate partial melting and fractional crystallization processes.

It is unlikely that eclogites and pyroxenites simultaneously were the sources of CVC rocks with a uniform chemical composition. According to the classification proposed by (Lambart et al., 2012; Lambart et al., 2016), these lithologies differ in silica saturation and the nature of the melts they produce. Silica-deficient pyroxenites are the source of nepheline-normative melts. On the other hand, eclogites are analogous to silica-excess pyroxenites and serve as a source of quartz-normative melts. Therefore, the following scenarios of melting modeling in pMELTS were considered:

— simultaneous melting of metasomatized peridotites and eclogites of CMLM;

— simultaneous melting of metasomatized peridotites and pyroxenites of CMLM.

Further, compositions were selected from the obtained melts to simulate fractional crystallization.

3.1. Selection of the chemical composition of starting materials

For the numerical simulations of the melting of metasomatized peridotites and pyroxenites/eclogites, the average compositions of the depleted mantle (DM) (e. g., McKenzie and O'Nions, 1991) and mid-ocean ridge basalts (MORBs) (e. g., Gale et al., 2013) can be used, respectively. However, although the main composition of peridotites is relatively homogeneous, the contents of Al_2O_3, FeO_{tot}, CaO, K_2O, and P_2O_5 in xenoliths of peridotites representing the CMLM of Mongolia (Carlson and Ionov, 2019; Kononova et al., 2002; Kourim et al., 2021; Wiechert et al., 1997) sometimes exceed the corresponding

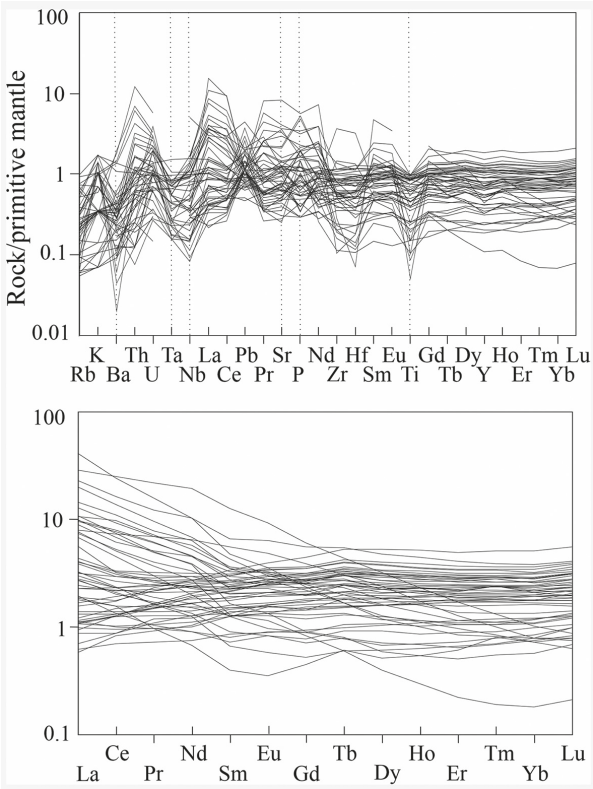

Fig. 2. Trace-element composition of CMLM peridotites from Mongolia (Carlson and Ionov, 2019; Kononova et al., 2002; Kourim et al., 2021; Wiechert et al., 1997)

values in DM. In addition, the above researchers' data show that Mongolia's CMLM is sometimes enriched in LILEs and LREEs, and depleted in HFSEs compared to DM peridotites. The eclogites/pyroxenites of Mongolia and the CAOB may also differ in their chemical composition from the average composition of MORBs. Sometimes, these rocks are significantly enriched in TiO_2, Al_2O_3, FeO_{tot}, CaO, Na_2O, K_2O, P_2O_5, LILEs, and LREEs (Ancuta et al., 2017; Barry et al., 2003; Gianola et al., 2019; Saktura et al., 2017; Stosch et al., 1995; Xu et al., 2009). To get results that are more consistent with the real ones, we use the CMLM compositions of Mongolia and the CAOB during the modeling of the formation mechanisms of the considered volcanic rocks. The compositions most enriched in incompatible trace elements were selected. We assume that this approach helps to determine whether the formation of CVC rocks with the participation of the most enriched peridotites, pyroxenites, and eclogites is possible.

It was revealed that most CMLM peridotite xenoliths have negative Ba, Nb, Ta, and Ti anomalies on the primitive mantle-normalized diagrams (Fig. 2). In addition, it can be seen that many of the CMLM peridotites of Mongolia are enriched in Th and U. There are compositions enriched with LREEs among the samples. The last criterion was one of the keys in selecting samples for modeling in pMELTS. As a result, a sample S-16 of spinel lherzolite was selected (Appendix 1) (Carlson and Ionov, 2019).

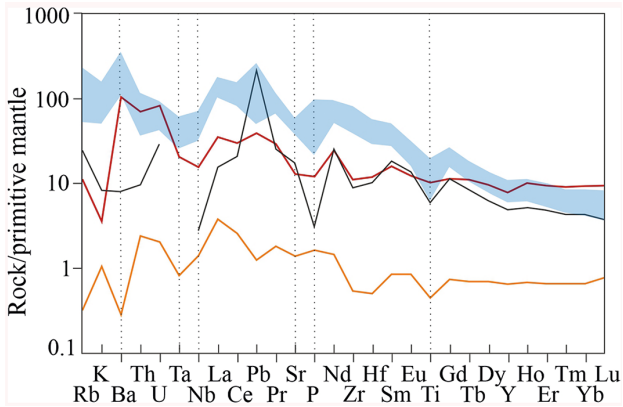

Fig. 3. Trace element composition of the CMLM rocks used in pMELTS modeling. The blue field is a range of the primitive mantle-normalized trace element contents for the CVC of the EMVA. The red line — eclogite JG2-2 (Xu et al., 2009), the black line — pyroxenite L4 (Xu et al., 2009), the orange line — lherzolite S-16 (Carlson and Ionov, 2019)

To date, there is no information in the literature about the findings of xenoliths in the territory of Mongolia represented by pyroxenites or eclogites. These rocks were described as a part of exhumed complexes representing relics of the mantle or Moho (Gianola et al., 2019; Skuzovatov, 2021). However, there is little information in the above sources about the chemical composition of these rocks. Also, these rocks are characterized by a relatively high content of SiO_2 (> 51 wt.%). Therefore, the rock compositions of the Xuzhou-Suzhou pyroxenite-eclogite complex in Central China were used in the modeling. These rocks represent either relics of subducted oceanic crust (Saktura et al., 2017) or relics of the North China Craton basement (Xu et al., 2009). Therefore, compositions of pyroxenite L4 and eclogite JG2-2 xenoliths were selected (Xu et al., 2009). Garnet, clinopyroxene, and amphibole are the main minerals of these rocks. However, sample JG2-2 also contains plagioclase, rutile, titanite, and quartz. Sample JG2-2 is characterized by a lower content of SiO_2, MgO, K_2O and a higher content of TiO_2, Al_2O_3, FeO_{tot}, and P_2O_5 (Appendix 1). Both samples are enriched in REEs and depleted in HFSEs (Fig. 3). However, JG2-2 is also highly enriched in Ba, Th, and U.

It should be noted that the CMLM rocks have elevated H_2O contents compared to rocks of the depleted mantle. In the case of CMLM peridotites, the H_2O content can reach 3737 ppm (~0.37 wt.%) (Green et al., 2014; Turner et al., 2017; Xia et al., 2019). Eclogites can contain up to 3070 ppm H_2O (~0.31 wt.%) (Javoy, 1997; Katayama et al., 2006; Radu, 2018; Ragozin et al., 2014). Also, it is known that H_2O in the metasomatized peridotites of the mantle wedge is one of the main triggers for their melting (Kelley et al., 2010). Moreover, the melting degree of rocks becomes higher with increasing their H_2O content (Hirschmann et al., 2009; Kelley et al., 2010). In this regard, the content of H_2O in the CMLM lithologies was also considered during the modeling in pMELTS.

However, data in Appendix 1 shows that H_2O content was not determined in selected samples of lherzolite, pyroxenite, and eclogite. Therefore, for the lherzolite sample, the mean value of H_2O (0.161 wt.%) in the CMLM peridotites of Mongolia (Wiechert et al.,

1997; Lesnov et al., 2009) was used in modeling. The same value was used in the modeling of pyroxenite and eclogite melting.

It is worth noting that this paper does not consider melting modeling with CO_2 addition. First, this is since small CO_2 contents (< 1 wt%) in peridotites and eclogites have been recognized in generating silica-poor, magnesium-rich, strongly alkalic magmas such as kimberlites, melilitites, and nephelinites (Hirose, 1997; Dasgupta et al., 2007, 2013; Malik and Dasgupta, 2014). However, CVC rocks sometimes belong to the subalkaline series and contain > 48.5 wt.% SiO_2 and < 4.2 MgO wt.% (Bars et al., 2018; Dash et al., 2015; Kuznetsov et al., 2022; Sheldrick et al., 2020a; Yarmolyuk et al., 2020). Second, pMELTS is not calibrated for CO_2 (Ghiorso et al., 2002).

3.2. Determination of P-T parameters for the modeling

A case that includes a constant pressure value and a changing temperature value during the formation of parent melts (isobaric melting) was considered in the paper.

According to (Dash et al., 2015; Kuznetsov et al., 2022; Sheldrick et al., 2020a), the formation of CVC parental magmas in the upper mantle was triggered by heat flow of rising asthenosphere after delamination of the lower parts of the CMLM. Since the isotope features of CVC rocks do not testify to the role of the depleted component in their source (Bars et al., 2018; Dash et al., 2015; Kuznetsov et al., 2022; Sheldrick et al., 2020a; Yarmolyuk et al., 2020), we assume that the areas of magma genesis at the stage of volcanism formation were located at shallow depths in the CMLM far from the lithosphere-asthenosphere boundary. These suggestions are consistent with the conclusions of (Yücel et al., 2017; Kolb et al., 2012) that alkaline magmas generally form due to the high melting degree of the lithospheric mantle at a shallower depth during ongoing lithospheric thinning and associated asthenospheric upwelling. However, we need to appeal to the thickness estimates of the continental crust within Eastern Mongolia to understand what pressure values in the upper parts of the CMLM could have been.

According to (Zorin, 1999), the thickness of the continental crust in the studied region is 42.5–45 km. However, the crust was thicker after the closure of the Mongol-Okhotsk Ocean and the subsequent collision (Meng, 2003). Therefore, CVC parental melts could be produced at higher depths. Nevertheless, the most intensive extensional deformations in the region occurred between 130 Ma and 120 Ma (Daoudene et al., 2013). According to the most reliable $^{40}Ar/^{39}Ar$ dating estimates, the peak of EMVA volcanism was at 120.7 (Sheldrick et al., 2020a) or 114 Ma (Dash et al., 2015). The results of K-Ar dating indicate that some volcanic fields of CVC were formed even later at 100 Ma (Kuznetsov et al., 2022; Yarmolyuk et al., 2020). Therefore, we can conclude that most CVC magmas formed after the main phase of the extension at the depths close to contemporaneous (Zorin, 1999).

If we assume the continental crust is homogeneous (granitic) in composition with an average mass of 2691 kg/m^3 (Aqua-Calc, 2023), the pressure under one cubic kilometer of the continental crust rocks will be 0.2637 kbar. Considering the estimates of the continental crust thickness in the region (Zorin, 1999), the approximate pressure at the boundary of the crust and the mantle is 11.2–11.9 kbar. Therefore, the pressure in the upper horizons of the CMLM was more than 12 kbar in the Late Mesozoic. We use P = 13 kbar in the thermodynamic modeling of rock melting in pMELTS.

The temperature range of 1200–1300 °C was chosen for melting modeling. This is because of the following reasons. First, the isotopic and geochemical features of CVC rocks show the role of the CMLM in their formation and exclude the participation of deep mantle sources (Bars et al., 2018; Dash et al., 2015; Kuznetsov et al., 2022; Sheldrick et al., 2020a; Yarmolyuk et al., 2020). Thus, the role of the mantle plume is unlikely at the stage of CVC formation. Therefore, the temperature of the formation of the parental melt in the CMLM is less than the temperature of the asthenospheric mantle, which, according to (Hamza and Vieira, 2012), is 1280–1480 °C. Second, at P = 13 kbar and T< 1200 °C, only andesitic melts are formed during the melting of the mafic lithologies (Klemme et al., 2002; Lambart et al., 2013; Pertermann and Hirschmann, 2003; Takahashi et al., 1998). Third, at P = 13 kbar and T > 1300 °C, the resulting melts are not enriched in incompatible trace elements because of the high degree of rock melting. However, one of the main features of CVC rocks is their significant enrichment in trace elements, exceeding the OIBs level (Bars et al., 2018; Dash et al., 2015; Kuznetsov et al., 2022; Sheldrick et al., 2020a; Yarmolyuk et al., 2020).

3.3. Selection of distribution coefficients for the melting modeling

To get reliable modeling results for trace elements, it is necessary to ensure that the program uses the correct distribution coefficients ($^{mineral/melt}D$). The default $^{mineral/melt}D$ values of pMELTS are calculated based on experimental data on the peridotites melting with the formation of basaltic composition melts (McKenzie and O'Nions, 1991; 1995). At the same time, the experiments data on the melting of mafic lithologies at P<15 kbar (Klemme et al., 2002; Lambart et al., 2013; Pertermann and Hirschmann, 2003; Qian and Hermann, 2013) indicate that basalt — basaltic andesite — andesite melts can form. However, to date, $^{mineral/melt}D$ values have been most thoroughly studied only for the "mineral — andesite melt" system (Bedard, 2006; Klemme et al., 2002; Pertermann and Hirschmann, 2003; Qian and Hermann, 2013).

To determine how much the simulation results will differ when using different $^{mineral/melt}D$, melting modeling of the mean MORB composition (Gale et al., 2013) was carried out at P = 13 kbar, T = 1200, 1250 and 1300 °C with an addition of 0.161 wt.% H_2O. In the first case, $^{mineral/melt}D$ values of (McKenzie and O'Nions, 1991; 1995) were used. In the second case, $^{mineral/melt}D$ values given in (Bedard, 2006) were used. It should be noted that the latter source provides the most complete data on $^{mineral/melt}D$ values for the "mineral–andesite melt" system during the melting of metabasites. The modeling results are shown in Fig. 4. It is noticeable that the normalized trace element contents mainly do not differ when using different $^{mineral/melt}D$ values. However, significant differences are observed in the HREEs area of spectra. This is because the $^{garnet/melt}D$ values for REEs, Ti, and Y given in (Bedard, 2006) are significantly higher than the pMELTS default coefficients. For example, according to (Bedard, 2006; McKenzie and O'Nions, 1991; 1995), $^{garnet/melt}D_{Lu}$ equals 24.1 and 5.5, respectively. Because garnet is a stable restite phase at T=1200 and 1250 °C, produced melts are strongly depleted in HREEs, Ti, and Y when modeling with $^{mineral/melt}D$ values of (Bedard, 2006). At T = 1300 °C, garnet is unstable, so the modeling results using different $^{mineral/melt}D$ values almost do not differ.

Considering that the modeling results with different $^{mineral/melt}D$ values have little differences, we use $^{mineral/melt}D$ values of (McKenzie and O'Nions, 1991; 1995) in pMELTS

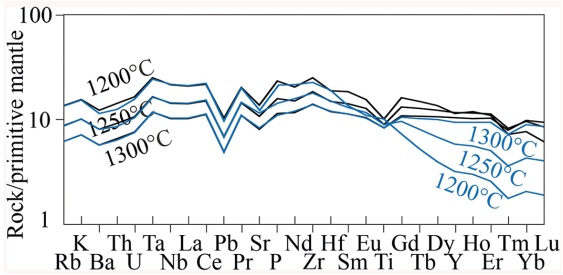

Fig. 4. Results of melting modeling of mean MORB composition (Gale et al., 2013) performed in pMELTS at P = 13 kbar, T = 1200, 1250, and 1300 °C with the addition of 0.161 wt.% H_2O. The black line — primitive mantle-normalized contents of trace elements obtained using pMELTS $^{mineral/melt}D$ values (McKenzie and O'Nions, 1991; 1995). The blue line — primitive mantle-normalized contents of trace elements obtained using $^{mineral/melt}D$ values from (Bedard, 2006)

Table 1. **$^{garnet/melt}D$ values used in pMELTS simulations**

Element	D	Element	D
P	0.142	Nd	0.1545
K	0.00115	Sm	0.8235
Ti	1.455	Eu	0.93
V	2.535	Gd	2.669
Co	2.0	Tb	4.275
Cr	13.75	Dy	6.28
Ni	1.2	Ho	8.415
Rb	0.0007	Er	10.4
Sr	0.0098	Tm	12.25
Y	8.105	Yb	13.615
Zr	0.4285	Lu	14.8
Nb	0.055	Hf	0.4355
Ba	0.0002	Ta	0.06
La	0.019	Pb	0.016
Ce	0.0505	Th	0.0045
Pr	0.102	U	0.0168

to model the melting of pyroxenite and eclogite. However, mean $^{mineral/melt}D$ values for garnet were used (Table 1). They are calculated using data from (McKenzie and O'Nions, 1991; 1995; Bedard, 2006).

3.4. pMELTS modeling strategy

The modeling of melting and mixing melts included three stages.

In the first stage, at a constant pressure (13 kbar) and varying temperature (1200–1300 °C), the melting of pyroxenite/eclogite was simulated using $^{garnet/melt}D$ values present-

ed in Table 1. The step of changing temperature was +10 °C. Then the program generated the main- and trace element composition of the resulting melt and coexisting residual mineral phases at each step of changing temperature.

In the second stage, the melting of peridotite was simulated following the same principles. However, the $^{garnet/melt}D$ values given in (McKenzie and O'Nions, 1991; 1995) were used in this case.

In the third stage, melts of different genesis obtained at the same pressure and temperature were mixed. To estimate correctly the chemical composition of the melts formed during mixing, it is necessary to understand the proportions in which the peridotites and eclogites/pyroxenites coexist in the CMLM. However, at present, there are no relevant data in the literature. Based on the fact that the isotopic composition of the studied volcanic rocks (Bars et al., 2018; Kuznetsov et al., 2022; Sheldrick et al., 2020a; Yarmolyuk et al., 2020) is strongly different from that of peridotites of the lithospheric mantle of Mongolia (Carlson and Ionov, 2019; Kononova et al., 2002; Kourim et al., 2021; Wiechert et al., 1997), this paper considers the melting of equal parts of peridotite and eclogite/pyroxenite substrates (1:1). Thus, the chemical composition of the melts formed during mixing was estimated using the formula:

$$C_{mix} = C_{pyr/ecl} \cdot F + C_{lh} \cdot (1 - F).$$

Where: C_{mix} — concentration of a given component in a hybrid melt; $C_{pyr/ecl}$ — concentration of a given component in the melt of pyroxenite/eclogite; C_{lh} — concentration of a given component in the melt of lherzolite; F — weight proportion of pyroxenite/eclogite melt, $(1 - F)$ — weight proportion of lherzolite melt.

4. Results of the pMELTS modeling

4.1. Composition of melts of selected samples

The results of the pMELTS melting modeling at P = 13 kbar and T = 1200–1300 °C of eclogite, pyroxenite, and lherzolite are presented in Fig. 5, 6.

The variation diagrams (Fig. 5) show that all modeled melts are depleted in K_2O and P_2O_5 compared to CVC rocks. However, it is worth noting that melts of eclogite at T~1200 °C are most similar in main composition to the studied rocks. The only difference is that eclogite-derived melts contain more FeO_{tot} (~18 wt.%), less MgO (~2 wt.%), K_2O (~0.3 wt.%), and P_2O_5 (~0.8 wt.%).

The lherzolite-derived melts correspond to CVC rocks concerning CaO and Na_2O contents. However, these melts are strongly depleted in TiO_2 and FeO_{tot} and rich in Al_2O_3. In turn, the pyroxenite-derived melts correspond to CVC rocks in terms of MgO only. The main feature of these melts is their silica-deficient composition.

The primitive mantle-normalized diagrams (Fig. 6) demonstrate that all modeled melts attend the enrichment levels of the studied rocks only at T~1200 °C. All spectra have negative anomalies of Ta and Nb, but both positive and negative anomalies of Sr and P. Significant Ti negative anomalies are observed in lherzolite- and pyroxenite-derived melts diagrams. In most cases, the modeled melts are far from the required enrichment levels for the most incompatible trace elements (Rb, K, Ba). Unlike lherzolite-derived melts, pyroxenite- and eclogite-derived melts at T = 1200 and 1250 °C have the slope of the spectra in the REEs area

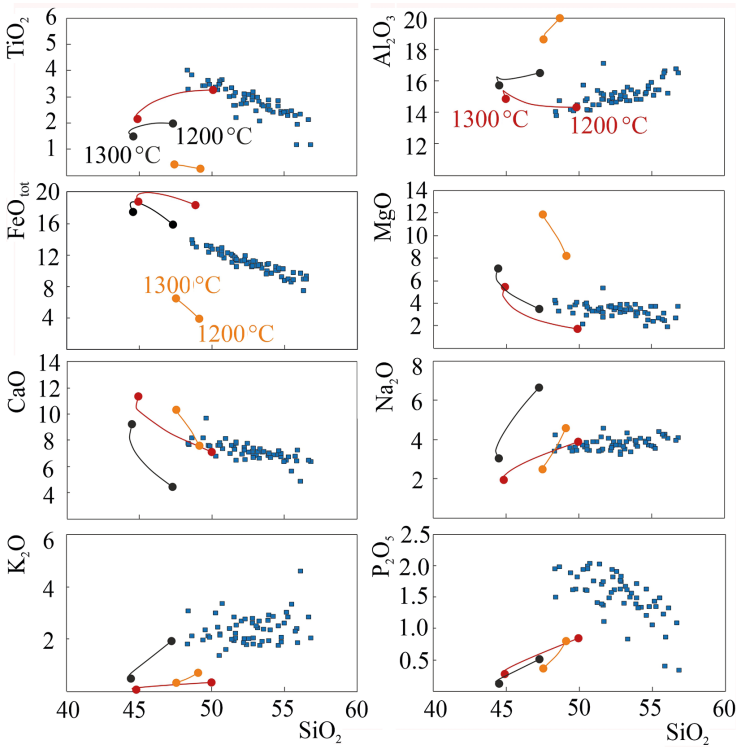

Fig. 5. Main components results (wt.%) of melting modeling in pMELTS (P = 13 kbar and T = 1200–1300 °C) of the rocks presented in Appendix 1. The red line depicts the evolution of JG2-2 eclogite-derived melts (Xu et al., 2009), the black line — L4 pyroxenite-derived melts (Xu et al., 2009), the orange line — S-16 lherzolite-derived melts (Carlson and Ionov, 2019). Blue squares — basaltic volcanic rocks of the CVC of the EMVA (Bars et al., 2018; Kuznetsov et al., 2022; Sheldrick et al., 2020a)

that coincides with that of CVC rocks. This is because garnet is one of the stable residual phases during the melting of mafic rocks at a given temperature range. During the melting of the spinel lherzolite, the composition of the melt is controlled by a spinel.

4.2. Composition of mixing (hybrid) melts

Fig. 7 and 8 show the results of the mixing modeling of CMLM-derived melts. It can be seen that the mixing melts slightly differ in chemical composition from the pure melts of pyroxenite or eclogite. The reason for this is the high melting degree of these rocks compared to peridotites. According to the melting modeling results, at T = 1200 °C, the melting degree of the eclogite is 0.29, the pyroxenite is 0.12, and the lherzolite is 0.04.

As expected, during the mixing of eclogite- and lherzolite-derived melts at T<1250 °C, the resulting melts are more similar in the main composition to the studied rocks relative to hybrids with pyroxenite-derived melts (Fig. 7). The spider diagrams show that the mixing of eclogite- and lherzolite-derived melts does not lead to the required enrichment in trace elements, even at T = 1200 °C (Fig. 8). Another difference between the compositions of modeled melts and CVC rocks is a significant depletion in fluid-mobile components

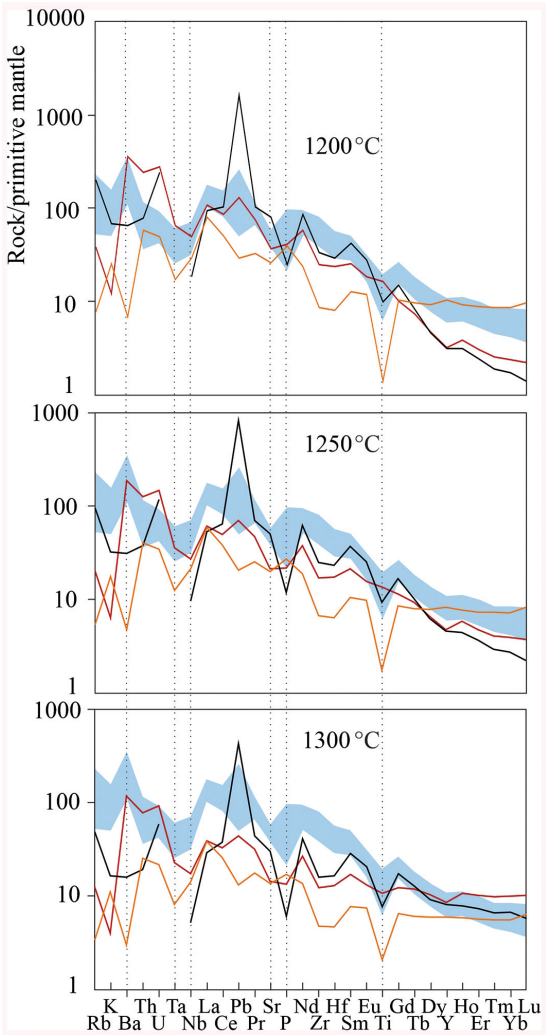

Fig. 6. Trace elements results of melting modeling in pMELTS (P = 13 kbar and T = 1200–1300 °C) of the CMLM rocks presented in Appendix 1. The red line — JG2-2 eclogite-derived melts (Xu et al., 2009), the black line — L4 pyroxenite-derived melts (Xu et al., 2009), the orange line — S-16 lherzolite-derived melts (Carlson and Ionov, 2019). The blue field is a range of the primitive mantle-normalized trace element contents for the CVC of the EMVA

(Rb, K) of the former. However, hybrids with eclogite-derived melts are characterized by sufficient Ba enrichment.

Pyroxenite- and lherzolite-derived hybrids are less similar to CVC rocks. These hybrid melts are more silica-deficient and contain less TiO_2 and CaO (Fig. 7). At the same time, they are more enriched in Al_2O_3 and Na_2O. The levels of trace elements enrichment of these hybrids are comparable to that of eclogite- and lherzolite-derived hybrids (Fig. 8). However, the former are more enriched in Rb, K, Pb, Sr and less enriched in Ba, Nb, P, and Ti relative to latter. Generally, the primitive mantle-normalized diagrams of pyroxenite- and lherzolite-derived hybrids are similar in pattern to that of CVC rocks.

Thus, the results of mixing modeling show that all hybrid melts lack sufficient enrichment in many main and trace elements. However, the simultaneous melting of eclogites and peridotites of the CMLM is more suitable for CVC rocks forming. The lack of enrichment in some elements can be leveled during crystallization differentiation. To test whether it is possible to enrich hybrid melts during the fractional crystallization to the levels of the studied rocks, a simulation of this process was carried out in pMELTS. Most likely, extremely alkaline and silica-deficient compositions can be formed as a result of crystallization differentiation of pyroxenite- and lherzolite-derived hybrids. However, to confirm this assumption, we also modeled this process in pMELTS.

4.3. Modeling of crystallization differentiation

Modeling of crystallization differentiation was carried out as follows. We selected two compositions among the hybrid melts, which can evolve into the compositions of CVC rocks during fractional crystallization. The key criterion in choosing the starting melts was their MgO content. Since the MgO content at the first stages of crystallization

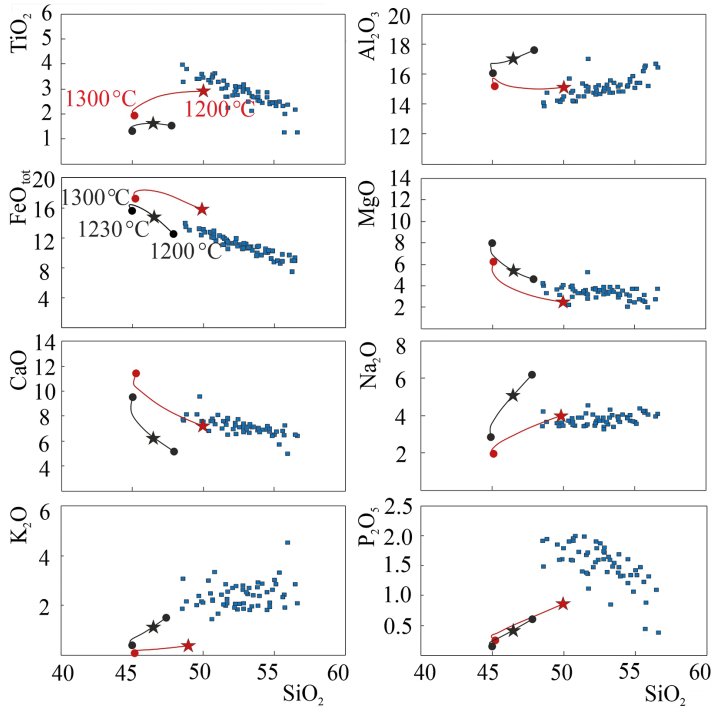

Fig. 7. The main composition of hybrid melts formed after the mixing of JG2-2 eclogite-derived melts (the red line) and L4 pyroxenite-derived melts (the black line) with S-16 lherzolite-derived melts at P = 13 kbar and T = 1200–1300 °C. The red asterisk depicts the composition of the eclogite-derived hybrid used in the modeling of crystallization differentiation. The black asterisk depicts the composition of the pyroxenite-derived hybrid used in the modeling of crystallization differentiation. The rest of the symbols are the same as in Fig. 5

differentiation is actively reduced during the fractionation of olivine, its content should be sufficient to form rocks with a magnesian number and trace elements enrichment similar to these in CVC rocks. Therefore, for modeling, it is necessary to choose compositions containing over 4.2 wt.% MgO (the highest value in CVC rocks).

The eclogite-derived hybrids (Fig. 7) with >4 wt.% MgO have much lower contents of the other main components than CVC rocks. For example, when MgO content is ~5 wt.%, SiO_2 content is ~45 wt.%, TiO_2 content is ~2 wt.%. This may indicate that the crystallization differentiation of eclogite-derived hybrids cannot lead to the formation of melts that correspond to CVC rocks in all main components. It is already possible to cease the simulation of this mechanism in pMELTS at this stage. However, it is necessary to determine whether crystallization differentiation can lead to the required enrichment in trace elements. To model this process, the hybrid composition obtained at T = 1200 °C was used. It is marked with a red asterisk in Fig. 7 and a bold red line in Fig. 8. Despite this composition having low MgO content, it corresponds most closely to the studied rocks in terms of the content of most main components and the pattern of distribution and enrichment of trace elements.

The pyroxenite-derived hybrids formed at T = 1200 °C contain more MgO than the CVC rocks. At the same time, these melts are not as silica-deficient as the eclogite-

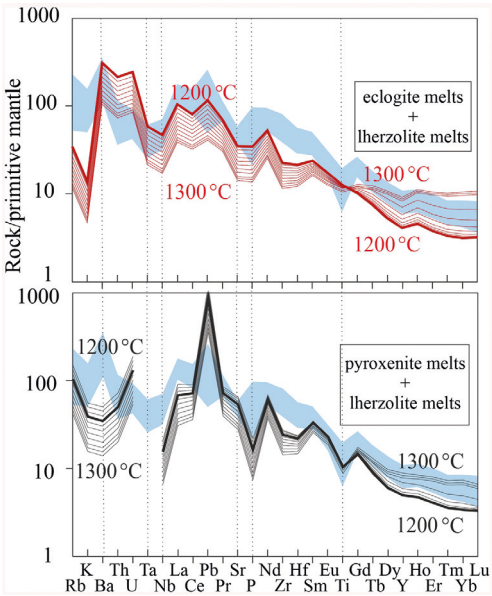

Fig. 8. Trace elements composition of hybrid melts obtained after the mixing of CMLM-derived melts at P = 13 kbar and T = 1200–1300 °C. Each line represents a 10 °C change in temperature. Bold lines depict compositions of hybrids chosen for modeling of crystallization differentiation. The blue field is a range of the primitive mantle-normalized trace element contents for the CVC of the EMVA

derived hybrids. Therefore, to simulate the process of crystallization differentiation in pyroxenite-derived hybrids, the composition obtained at T = 1230 °C was used (MgO = 5.45 wt.%). This composition is marked with a black asterisk in Fig. 7 and a bold black line in Fig. 8.

During the modeling of crystallization differentiation in pMELTS, a starting temperature corresponded to a temperature at which a particular hybrid melt was initially formed. The temperature step was –10 °C. pMELTS generated the main and trace element composition of the fractionated mineral phases and the remaining melt at each step of decreasing temperature. The process of crystallization differentiation was modeled for each hybrid melt at P = 5 and 1 kbar (the middle and upper continental crust levels, respectively). The $^{mineral/melt}D$ values given in (McKenzie and O'Nions, 1991; 1995) were used.

The results of the crystallization differentiation modeling show that the mixing of pyroxenite- and lherzolite-derived melts cannot be responsible for the formation of CVC rocks. Fig. 9 and 10 show that these melts become more silica-deficient and alkaline during their evolution in the continental crust.

As expected, the differentiates of eclogite-derived hybrids have low MgO content relative to CVC rocks. Only the Na_2O content in these melts approaches the corresponding values in CVC rocks both at P = 5 kbar and P = 1 kbar (Fig. 9 and 10). At P = 5 kbar, the differentiates have the same CaO content as the studied rocks. In both cases, P_2O_5 content in melts increases sharply to the levels of CVC basaltic trachyandesites in the first stages of crystallization differentiation. However, neither the melting of P_2O_5-rich mantle lithologies nor the process of crystallization differentiation can lead to the formation of the most primitive studied rocks regarding P_2O_5 content. The mechanism of crystallization differentiation of eclogite-derived hybrids at different pressures does not lead to the necessary enrichment in TiO_2 and K_2O. In addition, the differentiates are excessively rich in FeO_{tot} as well as their parental melts.

In contrast to the results for main components, the trace elements results of crystallization differentiation modeling show that the mixing of lherzolite- and pyroxenite-derived melts can form compositions like those of CVC rocks. Fig. 11 shows that the enrichment levels in trace elements of these differentiates sometimes even exceed the levels of the studied rocks. Moreover, the spider diagrams pattern of these differentiates almost wholly corresponds to that of studied volcanic rocks. The only difference is an insufficient enrichment in Ba and excessive enrichment in Th and U. An insignificant difference is also more

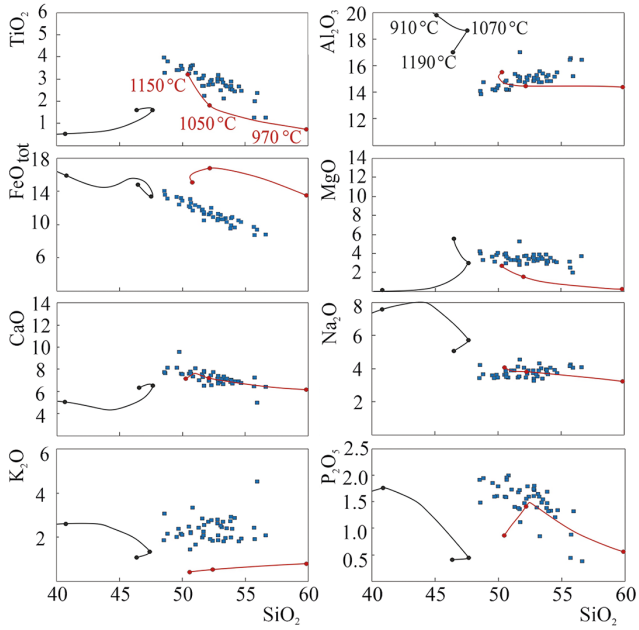

Fig. 9. The main component results of the crystallization differentiation modeling of lherzolite- and eclogite-derived hybrids (the red line) and lherzolite- and pyroxenite-derived hybrids (the black line) at P = 5 kbar. The rest of the symbols are the same as in Fig. 5

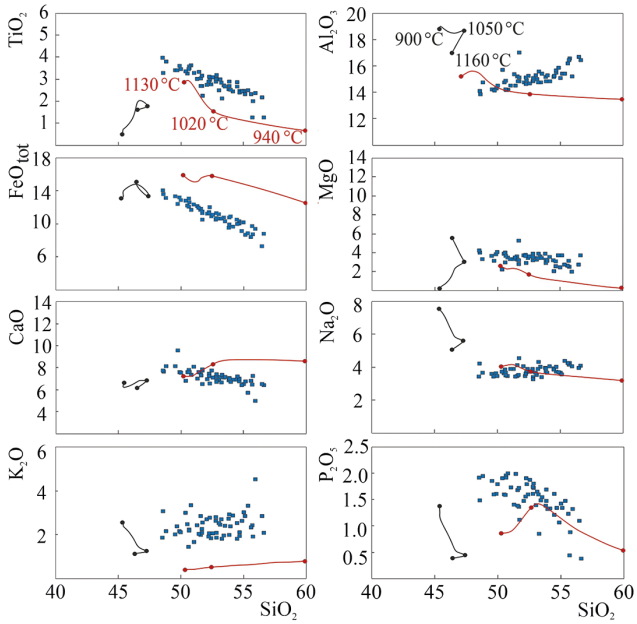

Fig. 10. The main component results of the crystallization differentiation modeling of lherzolite- and eclogite-derived hybrids (the red line) and lherzolite- and pyroxenite-derived hybrids (the black line) at P = 1 kbar. The rest of the symbols are the same as in Fig. 5

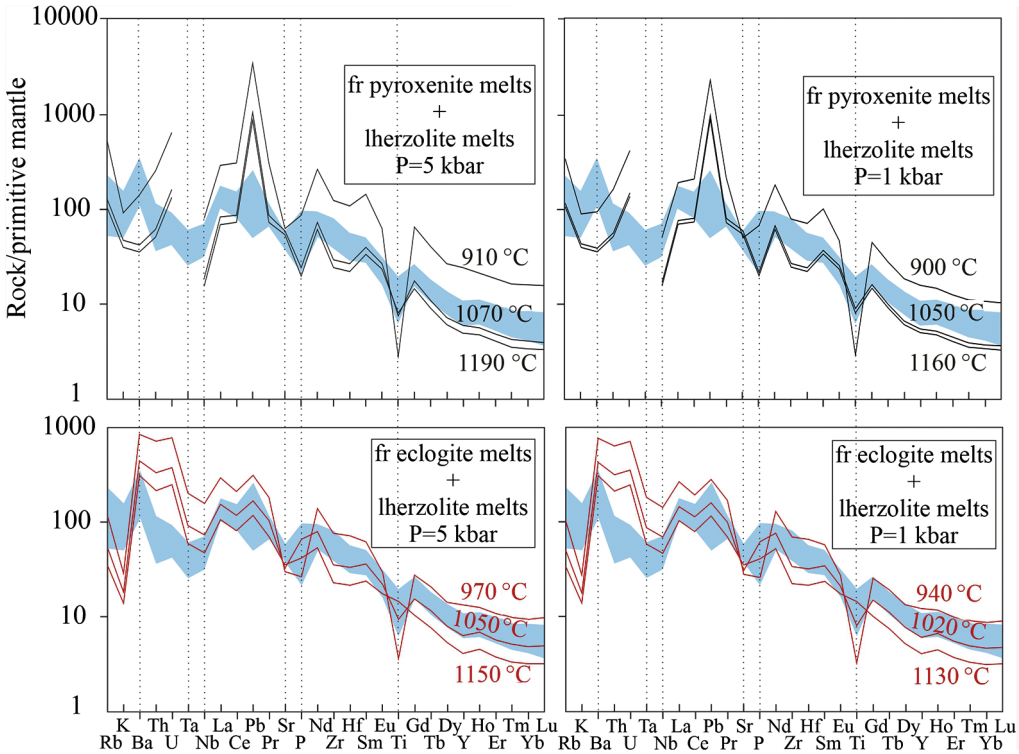

Fig. 11. Trace element results of crystallization differentiation modeling of lherzolite- and eclogite-derived hybrids and lherzolite- and pyroxenite-derived hybrids at P = 5 kbar and P = 1 kbar. The blue field is a range of the primitive mantle-normalized trace element contents for the CVC of the EMVA

pronounced negative Zr and Hf anomalies in the spectra of the differentiates. The degree of the spectra slope in the REEs area also corresponds to that in the studied volcanic rocks.

Modeling results for eclogite-derived hybrids also indicate that crystallization differentiation can lead to trace elements enrichment in them to the level of CVC rocks (Fig. 11). The spider diagrams pattern of the differentiates is very similar to that of studied volcanic rocks. There is almost complete correspondence in the area of REE. However, the required levels of Rb, K, and Sr enrichment are not achieved. As in the case of differentiates of pyroxenite-derived hybrids, there is an excessive enrichment in Th and U. This is due to the fact that initially modeled compositions are enriched in these elements.

5. Discussion

5.1. Role of metasomatic veins in the volcanic rocks formation

An analysis of the modeling results allows us to conclude that the case of mixing of eclogite- and lherzolite-derived melts is most consistent with the studied rocks. At the same time, this process does not produce magmas, which completely correspond in chemical composition to the basalts of the CVC. Thus, the modeling results of melting and crystallization differentiation using the most enriched CMLM compositions in incom-

patible elements indicate that melts with the required enrichment of Ti, K, P, Rb, and Sr are not formed. Therefore, besides metasomatized peridotites and eclogites, other CMLM rocks were involved in the formation of CVC rocks.

Positive P and Ba anomalies in the primitive mantle-normalized trace element spectra of CVC basalts (Kuznetsov et al., 2022; Sheldrick et al., 2020a; Yarmolyuk et al., 2020) may reflect the involvement of phlogopite- and apatite-bearing mantle metasomatic veins during magma generation processes (Kontak et al., 2001). J. Bedard and autors (Bedard et al., 2021) pointed out that the formation of alkaline rocks of the High Arctic igneous province in Canada enriched in TiO_2 (3–4 wt.%), K_2O (~ 3 wt.%), and P_2O_5 (~ 1.5 wt.%) resulted from melting of mantle metasomatic lithology of mainly pyroxenite composition with such additional mineral phases as apatite, rutile, and phlogopite. CVC rocks sometimes contain even more TiO_2 and P_2O_5 (Bars et al., 2018; Dash et al., 2015; Kuznetsov et al., 2022; Sheldrick et al., 2020a; Yarmolyuk et al., 2020). G. Farmer and autors (Farmer et al., 2020) came to a similar conclusion about the role of rutile- and apatite-bearing CMLM in forming mafic continental rocks of the Sierra Nevada and Rio Grande Rift with Ta/Th ratio between 0.2 and 0.6. This ratio varies from 0.23 to 0.52 in CVC basalts (Kuznetsov et al., 2022; Sheldrick et al., 2020a; Yarmolyuk et al., 2020).

S. O'Reilly and W. Griffin (O'Reilly and W. Griffin, 2013) concluded that magmas highly enriched in Sr, P, and K could only be produced by melting of metasomatized peridotites with a significant content of apatite and phlogopite + amphibole, respectively. Furthermore, experiments on the melting of the phlogopite-bearing peridotite (Condamine and Medard, 2014) show the formation of melts rich in K (3.05–6.68 wt.%) and Ti (0.29–1.45 wt.%). In turn, melts containing up to 5 wt.% TiO_2 can be formed during the melting of the substrate consisting of clinopyroxene and amphibole (Pilet et al., 2008). In addition, the studies of veins in peridotite massifs also testify to the role of atypical mantle rocks and minerals in the origin of K-rich magmas. Veins of the lithospheric mantle may be represented by glimmerites, the main minerals of which could be phlogopite and apatite (Becker et al., 1999). These rocks have high K_2O (up to 9.13 wt.%) and Rb content (up to 879 ppm), which suggests that their melting could produce melts enriched in these elements.

Thus, the lack in Ti, K, P, and sometimes Rb and Sr of eclogite- and lherzolite-derived hybrid melts relative to studied rocks requires participation in the volcanic rocks' formation of other CMLM lithologies (metasomatic veins) enriched with rutile, apatite, phlogopite, and amphibole. What could be the origin of these metasomatic veins? Considering that CVC rocks have high LILE/HFSE and LREE/HREE ratio values, we can conclude that the formation of veins in the CMLM could be related to previous subduction processes (Pearce et al., 2005). This conclusion is consistent with the fact that the territory of Eastern Mongolia was involved in subduction processes until the end of the Early Mesozoic (Arzhannikova et al., 2022; Yarmolyuk et al., 2019).

It should be noted that the melting modeling of metasomatic lithologies is associated with specific difficulties. For example, when selecting the starting materials representing metasomatized peridotites, pyroxenites, or eclogites, we can refer to the compositions of these rocks that are common within the region. However, this is not possible with other metasomatic formations since the volume of one mineral in metasomatic veins may vary significantly. Therefore, it is difficult to determine which minerals should be chosen for modeling and in what proportions they should be used. Nevertheless, the data of the

melting modeling of the enriched in trace element CMLM lithologies lead us to the conclusion that rutile-, apatite-, phlogopite-, and amphibole-bearing metasomatic veins were involved in the magma generation processes.

6. Conclusion

Thermodynamic modeling using pMELTS showed that the mixing of peridotite- and eclogite-derived melts corresponds most closely to the formation mechanism of Early Cretaceous rocks of the CVC of Eastern Mongolia. However, the lack in Ti, K, P, Rb, and Sr of the hybrid melts requires participating in magma generation processes of mantle metasomatic veins enriched with rutile, apatite, phlogopite, and amphibole. Thus, it could be concluded that peridotites, eclogites, and metasomatic veins of the CMLM were the sources of the studied rocks.

References

Aqua-Calc (2023). [online] Available at: https://www.aqua-calc.com/calculate/volume-to-weight/substance/granite-coma-and-blank-solid [Accessed 05.04.2023].

Ancuta, L. (2017). *Toward an Improved Understanding of Intraplate Uplift and Volcanism: Geochronology and Geochemistry of Intraplate Volcanic Rocks and Lower-Crustal Xenoliths*. PhD thesis. Lehigh University, Bethlehem.

Arzhannikova, A. V., Demonterova, E. I., Jolivet, M., Mikheeva, E. A., Ivanov, A. V., Arzhannikov, S. S., Khubanov, V. B., Kamenetsky, V. S. (2022). Segmental closure of the Mongol-Okhotsk Ocean: Insight from detrital geochronology in the East Transbaikalia Basin. *Geoscience Frontiers*, 13 (1), 1674–9871. https://doi.org/10.1016/j.gsf.2021.101254

Asimow, P. and Ghiorso, M. (1998). Algorithmic modifications extending MELTS to calculate subsolidus phase relations. *American Mineralogist.*, 83 (9–10), 1127–1132. https://doi.org/10.2138/am-1998-9-1022

Badarch, G., Cunningham, D., Windley, B. (2002). A new terrane subdivision for Mongolia: implications for the Phanerozoic crustal growth of Central Asia. *J. Asian Earth Sciences,* 21, 87–110. https://doi.org/10.1016/S1367-9120(02)00017-2

Barry, T., Saunders, A., Kempton, P., Windley, B., Pringle, M., Dorjnamjaa, D., Saandar, S. (2003). Petrogenesis of Cenozoic basalts from Mongolia: evidence for the role of asthenospheric versus metasomatized lithospheric mantle sources. *J. Petrology*, 44 (1), 55–91. https://doi.org/10.1093/petrology/44.1.55

Bars, A., Miao L., Fochin, Z., Baatar, M., Anaad, C., Togtokh, K. (2018). Petrogenesis and tectonic implication of the Late Mesozoic volcanic rocks in East Mongolia. *Willey Geology J.,* 53 (6), 1–22. https://doi.org/10.1002/gj.3080

Becker, H., Wenzel, T., Volker, F. (1999). Geochemistry of glimmerite veins in peridotites from Lower Austria — implications for the origin of K-rich magmas in collision zones. *J. Petrology*, 40 (2), 315–338. https://doi.org/10.1093/petroj/40.2.315

Bédard, J. A. (2006). A catalytic delamination-driven model for coupled genesis of Archean crust and sub-continental lithospheric mantle. *Geochimica et Cosmochimica Acta*, 70 (5), 1188–1214. https://doi.org/10.1016/j.gca.2005.11.008

Bédard, J., Troll, V., Deegan, F., Tegner, C., Saumur, B., Evenchick, C., Grasby, S., Dewing, K. (2021). High Arctic Large Igneous Province Alkaline Rocks in Canada: Evidence for Multiple Mantle Components. *J. Petrology*, 62 (9). https://doi.org/10.1093/petrology/egab042

Berman, R. G. (1988). Internally-consistent thermodynamic data for minerals in the system Na_2O-K_2O-CaO-MgO-FeO-Fe_2O_3-Al_2O_3-SiO_2-TiO_2-H_2O-CO_2. *J. Petrology*, 29 (2), 445–522. https://doi.org/10.1093/petrology/29.2.445

Carlson, R. and Ionov, D. (2019). Compositional characteristics of the MORB mantle and bulk silicate earth based on spinel peridotites from the Tariat Region, Mongolia. *Geochimica et Cosmochimica Acta*, 257, 206–223. https://doi.org/10.1016/j.gca.2019.05.010

Condamine, P. and Médard, E. (2014). Experimental melting of phlogopite-bearing mantle at 1 GPa: Implications for potassic magmatism. *Earth and Planetary Sciences Lett.*, 397, 80–92. https://doi.org/10.1016/j.epsl.2014.04.027

Daoudene, Y., Ruffet, G., Cocherie, A., Ledru, P., Gapais, D. (2013). Timing of exhumation of the Ereendavaa metamorphic core complex (north-eastern Mongolia) — U-Pb and $^{40}Ar/^{39}Ar$ constraints. *J. Asian Earth Sciences*, 62, 98–116. https://doi.org/10.1016/j.jseaes.2011.04.009

Dasgupta, R., Hirschmann, M. M., Smith, N. D. (2007). Partial melting experiments of peridotite + CO_2 at 3 GPa and genesis of alkalic ocean island basalts. *J. Petrology*, 48 (11), 2093–2124. https://doi:10.1093/petrology/egm053

Dasgupta, R., Mallik, A., Tsuno, K., Withers, A. C., Hirth, G., Hirschmann, M. M. (2013). Carbon-dioxide-rich silicate melt in the Earth's upper mantle. *Nature*, 493 (7431), 211–215. https://doi:10.1038/nature11731

Dash, B., Yinb, A., Jiang, N., Tseveendorj, B., Han, B. (2015). Petrology, structural setting, timing, and geochemistry of Cretaceous volcanic rocks in eastern Mongolia: Constraints on their tectonic origin. *Gondwana Research,* 27, 281–299. https://doi.org/10.1016/j.gr.2013.10.001

Farmer, G. L., Fritz, D. E., Glazner, A. F. (2020). Identifying Metasomatized Continental Lithospheric Mantle Involvement in Cenozoic Magmatism From Ta/Th Values, Southwestern North America. *Geochemistry, Geophysics Geosystems*, 21, e2019GC008499. https://doi.org/10.1029/2019GC008499

Gale, A., Dalton, C., Langmuir, C., Su, Y., Schilling, J.-G. (2013). The mean composition of ocean ridge basalts. *Geochemistry Geophysics. Geosystems*, 14, 489–518. https://doi.org/10.1029/2012GC004334

Ghiorso, M. and Sack, R. (1995). Chemical Mass-Transfer in Magmatic Processes IV. A Revised and Internally Consistent Thermodynamic Model for the Interpolation and Extrapolation of Liquid-Solid Equilibria in Magmatic Systems at Elevated-Temperatures and Pressures. *Contrib. Mineral. Petrol.*, 119 (2–3), 197–212. https://doi.org/10.1007/BF00307281

Ghiorso, M. S., Hirschmann, M. M., Reiners, P. W., Kress, V. C. (2002). The pMELTS: A revision of MELTS aimed at improving calculation of phase relations and major element partitioning involved in partial melting of the mantle at pressures up to 3 GPa. *Geochemistry Geophysics Geosystems*, 3 (5). https://doi.org/10.1029/2001GC000217

Gianola, O., Schmidt, M., Jagoutz, O., Rickli, J., Bruguier, O., Sambuu, O. (2019). The Crust–Mantle Transition of the Khantaishir Arc Ophiolite (Western Mongolia). *J. Petrology*, 60 (4), 673–700. https://doi.org/10.1093/petrology/egz009

Green, D., Hibberson, W., Rosenthal, A., Kovacs, I., Yaxley, G., Falloon, T., Brink, F. (2014). Experimental study of the influence of water on melting and phase assemblages in the upper mantle. *J. Petrology,* 55, 2067–2096. https://doi.org/10.1093/petrology/egu050

Hamza, V. and Vieira, F. (2012). Global distribution of the lithosphere-asthenosphere boundary: a new look. *Solid Earth*, 3, 199–212. https://doi.org/10.5194/se-3-199-2012

Hirose, K. (1997). Partial melt compositions of carbonated peridotite at 3 GPa and role of CO_2 in alkali-basalt magma generation. *Geophysical Research Lett.*, 24 (22), 2837–2840. https://doi.org/doi:10.1029/97gl02956

Hirschmann, M., Tenner, T., Aubaud, C., Withers, A. (2009). Dehydration melting of nominally anhydrous mantle: The primacy of partitioning. *Physics of the Earth and Planetary Interiors*, 176, 54–68. https://doi.org/10.1016/j.pepi.2009.04.001

Javoy, M. (1997) The major volatile elements of the Earth: Their origin, behavior, and fate. *Geophysical Research Lett.*, 24 (2), 177–180. https://doi.org/10.1029/96GL03931

Katayama, I., Nakashima, S., Yurimoto, H. (2006). Water content in natural eclogite and implication for water transport into the deep upper mantle. *Lithos*, 86 (3–4), 245–259. https://doi.org/10.1016/j.lithos.2005.06.006

Kelley, K., Plank, T., Newman, S., Stolper, E., Grove, T., Parman, S., Hauri, E. (2010). Mantle Melting as a Function of Water Content beneath the Mariana Arc. *J. Petrology*, 51 (8), 1711–1738. https://doi:10.1093/petrology/egq036

Klemme, S., Blundy, J., Wood, B. (2002). Experimental constraints on major and trace element partitioning during partial melting of eclogite. *Geochimica et Cosmochimica Acta*, 66, 3109–3123. https://doi.org/10.1016/S0016-7037(02)00859-1

Kolb, M., Paulick, H., Kirchenbaur, M., Münker, C. (2012). Petrogenesis of mafic to felsic lavas from the Oligocene Siebengebirge volcanic field (Germany): implications for the origin of intracontinental volcanism in Central Europe. *J. Petrology*, 53, 2349–2379. https://doi.org/10.1093/petrology/egs053

Kononova, V., Kurat, G., Embey-Isztin, A., Petrov, V. A., Koeberl, C., Brandstatter, F. (2002). Geochemistry of metasomatised spinel peridotite xenoliths from the Dariganga Plateau, South-eastern Mongolia. *Mineralogy and Petrology*, 75, 1–21. https://doi.org/10.1007/s007100200012

Kontak, D., Jensen, S., Dostal, J., Archibald, D., Kyser, T. (2001). Cretaceous mafic dyke swarm, Peary Land, Northernmost Greenland: geochronology and petrology. *The Canadian Mineralogist*, 39, 997–1020. https://doi.org/10.2113/gscanmin.39.4.997

Kourim, F., Wang, K.-L., Beinlich, A., Chieh, C.-J., Dygert, N., Lafay, R., Kovach, V., Michibayashi, K., Yarmolyuk, V., Iizuka, Y. (2021). Metasomatism of the off-cratonic lithospheric mantle beneath Hangay Dome, Mongolia: Constraints from trace-element modeling of lherzolite xenoliths. *Lithos*, 400–401. https://doi.org/10.1016/j.lithos.2021.106407

Kuznetsov, M. V., Savatenkov, V. M., Shpakovich, L. V., Yarmolyuk, V. V., Kozlovsky, A. M. (2022). Evolution of the Magmatic Sources of the Eastern Mongolian Volcanic Area: Evidence from Geochemical and Sr–Nd–Pb Isotope Data. *J. Petrology*, 30 (5), 457–479. https://doi.org/ 10.1134/S0869591122050034

Kuznetsov, M. V., Savatenkov, V. M., Sheldrick, T., Shpakovich, L. V. (2023). Early Cretaceous trachytes and basement rocks from northeastern Mongolia: A Sr-Nd-Pb isotope study. *Frontiers of Earth Science* 11:1156559. https://doi.org/10.3389/feart.2023.1156559

Lambart, S., Laporte, D., Provost, A., Schiano, P. (2012). Fate of pyroxenite-derived melts in the peridotitic mantle: Thermodynamical and experimental constraints. *J. Petrology* 53 (3), 451–476. https://doi.org/10.1093/petrology/egr068

Lambart, S., Laporte, D., Schiano, P. (2013). Markers of the pyroxenite contribution in the major-element compositions of oceanic basalts: Review of the experimental constraints. *Lithos*, 160–161, 14–36. https://doi.org/10.1016/j.lithos.2012.11.018

Lambart, S., Baker, M. B., Stolper, E. M. (2016). The role of pyroxenite in basalt genesis: Melt-PX, a melting parameterization for mantle pyroxenites between 0.9 and 5 GPa. *J. Geophysical Research: Solid Earth*, 121, 5708–5735. https://doi.org/10.1002/2015JB012762

Lesnov, F. P., Kozmenko, O. A., Nikolaeva, I. V., Palesskii, S. V. (2009). Residence of incompatible trace elements in a large spinel lherzolite xenolith from alkali basalt of Shavaryn Tsaram-1 paleovolcano (western Mongolia). *Russian Geology and Geophysics*, 50 (12), 1063–1072. https://doi.org/10.1016/j.rgg.2009.11.005

Mallik, A. and Dasgupta, R. (2014). Effect of variable CO_2 on eclogite derived andesite and lherzolite reaction at 3 GPa — Implications for mantle source characteristics of alkalic ocean island basalts. *Geochemistry Geophysics. Geosystems*, 15, 1533–1557. https://doi.org/10.1002/2014GC005251

McKenzie, D. and O'Nions, R. K. (1991). Partial melt distributions from inversion of rare Earth element concentrations. *J. Petroogy*, 32, 1021–1091. https://doi.org/10.1093/petrology/32.5.1021

McKenzie, D. and O'Nions, R. K. (1995). The Source Regions of Ocean Island Basalts. *J. Petrology*, 36, 133–159. https://doi.org/10.1093/petrology/36.1.133

Meng, Q. R. (2003). What drove late Mezosoic extension of the northern China-Mongolia tract? Tectonophysics, 369 (3–4), 155–174. https://doi.org/10.1016/S0040-1951(03)00195-1

Miao, L., Zhang, F., Baatar, M., Zhu, M., Anaad, C. (2017). SHRIMP zircon U-Pb ages and tectonic implications of igneous events in the Ereendavaa metamorphic terrane in NE Mongolia. *J. Asian Earth Sciences,* 144, 243–260. https://doi.org/10.1016/j.jseaes.2017.03.005

O'Reilly, S. and Griffin, W. (2013). Mantle Metasomatism. In: D. Harlov, J. Austrheim, ed., *Metasomatism and the Chemical Transformation of Rock*. Heidelberg: Springer, 471–534.

Pearce, J., Stern, R., Bloomer, S., Fryer, P. (2005). Geochemical mapping of the Mariana arc-basin system: Implications for the nature and distribution of subduction components. *Geochemistry Geophysics. Geosystems*, 6, Q07006. https://doi.org/10.1029/2004GC000895

Peretyazhko I. S., Savina E. A., Dril' S. I. (2018). Early Cretaceous trachybasalt-trachyte-trachyrhyolitic volcanism in the Nyalga basin (Central Mongolia): sources and evolution of continental rift magmas. *Russian Geology. Geophysics*, 59 (12), 1679–1701. https://doi.org/10.1016/j.rgg.2018.12.011

Pertermann, M. and Hirschmann, M. (2003). Anhydrous Partial Melting Experiments on MORB-like Eclogite: Phase Relations, Phase Compositions and Mineral-Melt Partitioning of Major Elements at 2-3 GPa. *J. Petrology*, 44 (12), 2173–2201. https://doi.org/10.1093/petrology/egg074

Pilet, S., Baker, M., Stolper, E. (2008). Metasomatized lithosphere and the origin of alkaline lavas. *Science*, 320 (5878), 916–919. https://doi/10.1126/science.1156563

Qian, Q. and Hermann, J. (2013). Partial melting of lower crust at 10–15 kbar: Constraints on adakite and TTG formation. *Contrib. Mineral. Petrol.*, 165, 1195–1224. https://doi.org/10.1007/s00410-013-0854-9

Radu, I. (2018). Cratonic eclogite xenoliths — formation and evolution of the subcontinental lithospheric mantle. PhD thesis. University of Cape Town.

Ragozin, A. L., Karimova, A. A., Litasov, K. D., Zedgenizov, D. A., Shatsky, V. S. (2014). Water content in minerals of mantle xenoliths from the Udachnaya pipe kimberlites (Yakutia). *Russian Geology Geophysics*, 55 (4), 428–442, https://doi.org/10.1016/j.rgg.2014.03.002

Saktura, W., Buckman, S., Nutman, A., Belousova, E., Yan, Z., Aitchison, J. (2017). Continental origin of the Gubaoquan eclogite and implications for evolution of the Beishan Orogen, Central Asian Orogenic Belt, NW China. *Lithos*, 294–295, 20–38. https://doi.org/10.1016/j.lithos.2017.10.004

Sheldrick, T. C., Barry, T. L., Millar, I. L., Barfod, D. N., Halton, A. M., Smith, D. J. (2020a). Evidence for southward subduction of the Mongol-Okhotsk oceanic plate: Implications from Mesozoic adakitic lavas from Mongolia. *Gondwana Research.*, 79, 140–156. https://doi.org/10.1016/j.gr.2019.09.007

Sheldrick, T. C., Barry, T. L., Dash, B., Gan, C., Millar, I. L., Barfod, D. N., Halton, A. M. (2020b). Simultaneous and extensive removal of the East Asian lithospheric root. *Scientific Reports,* 10, 4128. https://doi.org/10.1038/s41598-020-60925-3

Sheldrick, T. C., Hahn, G., Ducea, M. N., Stoica, A. M., Constenius, K., Heizler, M. (2020c). Peridotite versus pyroxenite input in Mongolian Mesozoic-Cenozoic lavas, and dykes. *Lithos*, 376–377. https://doi.org/10.1016/j.lithos.2020.105747

Skuzovatov, S. (2021). Nature and (in-)coherent metamorphic evolution of subducted continental crust in the Neoproterozoic accretionary collage of SW Mongolia. *Geoscience Frontiers*, 12 (3), 101097. https://doi.org/10.1016/j.gsf.2020.10.004

Stosch, H., Ionov, D., Puchtel, I., Galer, S., Sharpouri, A. (1995). Lower crustal xenoliths from Mongolia and their bearing on the nature of the deep crust beneath central Asia. *Lithos*, 36(3), 227–242. https://doi.org/10.1016/0024-4937(95)00019-4

Takahashi, E., Nakajima, K., Wright, T. L. (1998). Origin of the Columbia River basalts: Melting model of a heterogeneous plume head. *Earth and Planetary Sciences Lett.*, 162, 63–80. https://doi.org/10.1016/S0012-821X(98)00157-5

Turner, M., Turner, S., Blatter, D., Maury, R., Perfit, M., Yogodzinski, G. (2017). Water contents of clinopyroxenes from sub-arc mantle peridotites. *Wiley Island Arc*, 26 (5). https://doi.org/10.1111/iar.12210

Wiechert, U., Ionov, D., Wedepohl, K. (1997). Spinel peridotite xenoliths from the Atsagin-Dush volcano, Dariganga lava plateau, Mongolia: a record of partial melting and cryptic metasomatism in the upper mantle. *Contrib. Mineral. Petrol.*, 126, 345–364. https://doi.org/10.1007/s004100050255

Xia, Q.-K., Liu, J., Kovács, I., Hao, Y.-T., Li, P., Yang, X.-Z., Chen, H., Sheng, Y.-M. (2019). Water in the upper mantle and deep crust of eastern China: concentration, distribution and implications. *National Science Review*, 6 (1), 125–144. https://doi.org/10.1093/nsr/nwx016

Xu, W., Gao, S., Yang, D.-B., Pei, F.-P., Wang, Q.-H. (2009). Geochemistry of eclogite xenoliths in Mesozoic adakitic rocks from Xuzhou-Suzhou area in central China and their tectonic implications. *Lithos*, 107, 269–280. https://doi.org/10.1016/j.lithos.2008.11.004

Yarmolyuk, V. V., Kozlovsky, A. M., Travin, A. V., Kirnozova, T. I., Fugzan, M. M., Kozakov, I. K., Plotkina, Yu. V., Eenzhin, G., Oyunchimeg, Ts., Sviridova, O. E. (2019). Duration of formation and geodynamic nature of giant batholiths of Central Asia: data of geological and geochronological studies Khangai batholith. *Stratigraphy. Geological correlation*, 27 (1), 79–102. https://doi.org/10.31857/0869-592X27179-102

Yarmolyuk, V. V., Kozlovskiy, A. M., Savatenkov, V. M., Kudryashova E. A., Kuznetsov M. V. (2020). Late Mesozoic Eastern Mongolia volcanic area: structure, magmatic associations, and sources of magmatism. *Petrology*, 28 (6), 563–590. https://doi.org/10.1134/S0869591120060053

Yücel, C., Arslan, M., Temizel, I., Yazar, E. A., Ruffet, G. (2017). Evolution of K-rich magmas derived from a net veined lithospheric mantle in an ongoing extensional setting: Geochronology and geochemistry of Eocene and Miocene volcanic rocks from Eastern Pontides (Turkey). *Gondwana Research*, 45, 65–86, https://doi.org/10.1016/j.gr.2016.12.016

Zorin, Yu. (1999). Geodynamics of the western part of the Mongol-Okhotsk collisional belt, Trans-Baikal region (Russia) and Mongolia. *Tectonophysics*, 306, 33–56. https://doi.org/10.1016/S0040-1951(99)00042-6

Received: January 16, 2023
Accepted: August 11, 2023

Authors' information:

Maksim V. Kuznetsov — garneteclogite@gmail.com
Valery M. Savatenkov — v.m.savatenkov@ipgg.ru

Моделирование процессов смешения расплавов перидотитового и мафического субстратов на малых глубинах континентальной метасоматизированной литосферной мантии. К вопросу о генезисе раннемелового вулканизма Восточной Монголии*

М. В. Кузнецов[1], *В. М. Саватенков*[1,2]

[1] Институт геологии и геохронологии докембрия Российской академии наук, Российская Федерация, 199034, Санкт-Петербург, наб. Макарова, 2
[2] Санкт-Петербургский государственный университет, Российская Федерация, 199034, Санкт-Петербург, Университетская наб., 7–9

Для цитирования: Kuznetsov, M. V., Savatenkov, V. M. (2023). Melting modeling of mixed peridotitic and mafic lithologies at shallow depths of the continental metasomatized lithospheric mantle: Implementation for the Early Cretaceous volcanic rocks of Eastern Mongolia. *Вестник Санкт-Петербургского университета. Науки о Земле*, 68 (3), 596–617. https://doi.org/10.21638/spbu07.2023.309

Восточно-Монгольская вулканическая область сформировалась в позднем мезозое — раннем кайнозое в пределах Центрально-Азиатского складчатого пояса. Основные вулканические события в области произошли в раннем мелу, когда щелочно-базальтоидные лавы сформировали так называемый покровный вулканический комплекс. Изотопно-геохимические особенности данного комплекса позволили исследователям установить следующие мантийные породы в качестве его источника: метасоматизированные перидотиты, эклогиты и пироксениты. Чтобы определить, действительно ли одновременное плавление данных пород с последующими процессами кристаллизационной дифференциации могло привести к формированию вулканитов, было проведено термодинамическое моделирование в программе alphaMELTS. Результаты моделирования свидетельствуют о том, что плавление наиболее обогащенных несовместимыми редкими элементами перидотитов, эклогитов и пироксенитов не могло формировать расплавы покровного вулканического комплекса. В то же время процессы смешения расплавов перидотитов и эклогитов в наибольшей степени соответствуют механизму формирования вулканитов. Однако обогащение вулканических пород Ti, K, P, Rb и Sr по отношению к моделируемым расплавам требует участия в процессах магмогенерации мантийных метасоматических жил, обогащенных рутилом, апатитом, флогопитом и амфиболом.

Ключевые слова: Восточная Монголия, раннемеловой вулканизм, термодинамическое моделирование, эклогиты, пироксениты, мантийные метасоматические жилы.

Статья поступила в редакцию 16 января 2023 г.
Статья рекомендована к печати 11 августа 2023 г.

Контактная информация:

Кузнецов Максим Викторович — garneteclogite@gmail.com
Саватенков Валерий Михайлович — v.m.savatenkov@ipgg.ru

* Эта работа была профинансирована Российским научным фондом (проект № 23-27-00165) и государственным заданием Института геологии и геохронологии докембрия Российской академии наук № FMUW-2022-0005.